C. R. Physique 12 (2011) 502–514

Contents lists available at ScienceDirect

Comptes Rendus Physique

www.sciencedirect.com

Superconductivity of strongly correlated systems / Supraconductivité des systèmes fortement corrélés

Studies of the gap structure of iron-based superconductors using magnetic penetration depth

Étude de la structure du gap des supraconducteurs à base de fer par la longueur de pénétration magnétique

Antony Carrington

H.H. Wills Physics Laboratory, University of Bristol, Tyndall Avenue, Bristol, BS8 1TL, United Kingdom

ARTICLE INFO

Article history:
Available online 14 May 2011

Keywords:
Iron-based superconductors
Iron-pnictide superconductors
Gap structure
Magnetic penetration depth

Mots-clés :
Supraconducteurs à base de fer
Supraconducteurs fer-pnictide
Structure de gap
Longueur de pénétration magnétique

ABSTRACT

This article reviews experiments to determine the structure of the superconducting gap in the iron-based superconductors. It focuses on insights provided by measurements of the temperature dependence of magnetic penetration depth but also discusses the information provided by other measurements especially thermal conductivity. The article includes background theory on the types of gap structure suggested for the iron-based superconductors as well as the general theory of penetration depth in conventional and unconventional superconductors. The effect of impurity scattering on each candidate gap structure is important for the interpretation of data and so will also be discussed. Penetration depth data for single crystals of the following compounds is reviewed: $SmFeAsO_{0.8}F_{0.2}$, $FeTe_{0.5}Se_{0.5}$, LaFePO, KFe_2As_2 and $BaFe_2(As_{0.67}P_{0.33})_2$ along with discussion on related materials such as K- and Co-doped $BaFe_2As_2$.

© 2011 Académie des sciences. Published by Elsevier Masson SAS. All rights reserved.

RÉSUMÉ

Cet article passe en revue des expériences visant à déterminer la structure du gap supraconducteur dans les supraconducteurs à base de fer. Il se focalise sur les informations obtenues par des mesures de la longueur de pénétration magnétique et de sa dépendance en température, mais les propriétés obtenues par d'autres moyens de mesures sont aussi examinées, en particulier la conductivité thermique. L'article comprend une description théorique de base sur les types de structures de gap suggérées pour les supraconducteurs à base de fer, ainsi que la théorie générale de la longueur de pénétration dans les supraconducteurs conventionnels et non conventionnels. L'effet de la diffusion des impuretés sur chacune des structures de gap candidates, important pour l'interprétation des données, sera également analysé. Les données de longueurs de pénétration des monocristaux des composés suivants sont examinées : $SmFeAsO_{0.8}F_{0.2}$, $FeTe_{0.5}Se_{0.5}$, LaFePO, KFe_2As_2 et $BaFe_2(As_{0.67}P_{0.33})_2$; des matériaux tels que $BaFe_2As_2$ dopé par K et Co seront aussi discutés.

© 2011 Académie des sciences. Published by Elsevier Masson SAS. All rights reserved.

E-mail address: a.carrington@bristol.ac.uk.

1631-0705/$ – see front matter © 2011 Académie des sciences. Published by Elsevier Masson SAS. All rights reserved.
doi:10.1016/j.crhy.2011.03.001

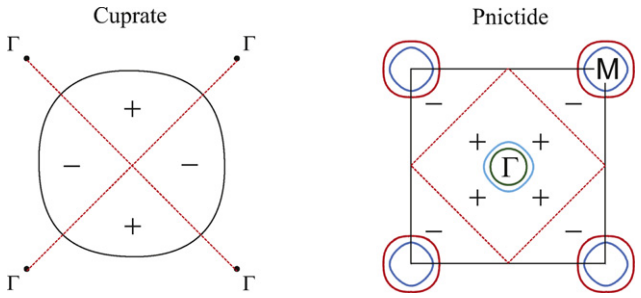

Fig. 1. Cross-sections of the Fermi surfaces of the cuprate superconductor $Tl_2Ba_2CuO_{6+\delta}$ [1,2] and the iron-pnictide superconductor LaFePO [3] along with a schematic showing the sign reversal of the gap function for the $d_{x^2-y^2}$ pairing state (cuprate) and $s_{\pm}$ pairing state (pnictide). The dashed line demarks the regions where the gap changes sign. For LaFePO the solid box is the Brillouin zone. This has been omitted from the $Tl_2Ba_2CuO_{6+\delta}$ figure for clarity. The letters (Γ, M) label the symmetry point of the Brillouin zone.

1. Introduction

Since the discovery of heavy fermion and high T_c cuprate superconductors it has been common to question whether the pairing interaction responsible for the superconductivity is the conventional one, as explained in the original BCS theory, or whether it is something else, for example it may be of magnetic or electronic origin. When a new superconducting material, or family of materials, is discovered one of the first questions asked concerns the symmetry and anisotropy of the superconducting gap (which is the superconducting order parameter). The reason for this is that this information is an essential first step along the road to establishing what is the mechanism of superconductivity in the material.

1.1. Pairing states

In the absence of complicating factors, the superconducting gap will have the same symmetry as the lattice, i.e., it will have *s* symmetry with Cooper pairs having zero angular momentum. In fact, in many cases, the scattering rate is sufficiently large that any intrinsic anisotropy of the gap, resulting from variations of the pairing potential $V_{kk'}$ across the Fermi surface, will be averaged out, so that the gap Δ will be isotropic (independent of k). The *s* pairing state will usually have the lowest energy (and hence highest T_c) because this makes maximum use of phase space (and electrons) available to be paired. However, if $V_{kk'}$ is repulsive in some or all directions then the gap may develop nodes or deep minima on certain sections of the Fermi surface. This may involve pairing the electrons in higher momentum states (e.g., $l = 2$, the *d* state). The nodes will generally occur where $V_{kk'}$ is most repulsive.

Although the BCS theory originally was used to explain phonon driven superconductivity, the majority of the formalism also applies to other sources of electron pairing, for example antiferromagnetic spin fluctuations. For a material to be superconducting there must be a solution to the BCS self-consistent gap equation [4]

$$\Delta_{k'} = -\sum_{k} V_{kk'} \frac{\Delta_k}{2(\varepsilon_k^2 + \Delta_k^2)^{\frac{1}{2}}} \tag{1}$$

where ε_k are the single electron energies. If $V_{kk'}$ is everywhere repulsive (positive) (as it is for some models of pairing via antiferromagnetic spin fluctuations [5]) then clearly a finite solution to Eq. (1) for Δ_k can only be found if Δ_k changes sign somewhere on the Fermi surface thereby making both sides of the equation positive. For two-dimensional single band materials, with a single sheet of Fermi surface, this will inevitably lead to nodes on the Fermi surface, with Δ changing sign at these points. However, if there is more than one Fermi surface sheet this is no longer the case as Δ could be isotropic on each sheet but have different sign on each of the sheets. This is illustrated in Fig. 1 where the experimentally determined Fermi surfaces of the high T_c cuprate superconductor $Tl_2Ba_2CuO_{6+\delta}$ and the iron-pnictide superconductor LaFePO are shown along with possible pairing states. For the cuprate superconductor the $d_{x^2-y^2}$ pairing state has nodes along the (110) directions and the sign of Δ is opposite for Cooper pairs travelling in the *x*- or *y*-directions respectively. Hence this state has a lower symmetry than the tetragonal crystal lattice. The situation for LaFePO is quite different. Here, a pairing state has been proposed [6,7] which has no nodes but which changes sign between the electron (at the zone corner M) and hole (at the zone centre Γ) sheets of Fermi surface. This type of pairing state is know as an $s_{\pm}$ state, reflecting the fact that it does not break the crystal symmetry (rotating it by $\pi/2$ results in the same pattern), but is different from the conventional *s* state where there is no sign changing. It can be seen that in both cases, Δ changes sign for states connected by the vector (π, π) (in reciprocal lattice units), which in the simplest case is the wave-vector at which the spin-susceptibility (which is proportional to the strength of the spin-fluctuations assumed to be causing the pairing) is maximum.

Soon after the explosion of research which followed the discovery of high temperature superconductivity (T_c up to 55 K) in iron-pnictides, it was proposed that the pairing state of this materials would predominately be of the $s_{\pm}$ type outlined above. This conclusion was based on the assumption that spin-fluctuations provided the pairing interaction, and that the strength of these spin-fluctuations would be strong peaked at a wave-vector of (π, π). This latter assumption was based

on the observation that the Fermi surfaces of the iron-pnictides are close to fulfilling a nesting condition. That is to say that a wave-vector $\mathbf{Q}_0 = (\pi, \pi)$ approximately connects all the states on one of the hole sheets to a corresponding state on one of the electron sheets. Perfect nesting would likely result in an electronic instability leading to magnetically ordered spin-density wave ground state, whereas imperfect nesting results in a strong broad peak in the dynamic spin susceptibility $\chi(\boldsymbol{q})$ at $\boldsymbol{q}$ close to $\mathbf{Q}_0$ which can lead to a superconducting ground state [6,7].

Although, the position, shape and size of the Fermi surface sheets in iron-pnictides (typified for the 1111 phases by the Fermi surface of LaFePO shown in Fig. 1), are strongly suggestive of nesting leading to a peak in $\chi(\boldsymbol{q})$ at $\boldsymbol{q} = \mathbf{Q}_0$, more detailed calculations show there is further structure in $\chi(\boldsymbol{q})$ which can lead to other pairing channels being favoured over the simple $s_{\pm}$ state [8–10]. First of all, transitions between the two electron or two hole sheets give an enhancement of $\chi(\boldsymbol{q})$ at small $\boldsymbol{q}$, and the other contributions $\chi(\boldsymbol{q})$ are modified by the different band-characters of the various sheet. For example, in LaFePO, the outer electron sheet comes from the Fe d_{xy} orbitals whereas the inner hole sheet has strong Fe d_{xz} character. The matrix element connecting these states is small and hence these states will not contribute strongly to $\chi(\boldsymbol{q})$. A detailed calculation of both the non-interacting susceptibility (including matrix element effects) and the interacting susceptibility using the random phase approximation has been performed by Graser et al. [8]. They concluded that the resulting form of $\chi(\boldsymbol{q})$ favours two pairing states which are quasi-degenerate. Both have nodes on one or more of the Fermi surface sheets. One of the states has s-symmetry and the other d-symmetry. Clearly, according to this theory (and assuming that spin fluctuations are the pairing force), small changes in the Fermi surface topology (or character) could have a marked effect on determining which particular pairing state that has the lowest energy. So it is possible or even likely, that the pairing state of the iron-based superconductors will not all be the same. Similar conclusions, as to the existence of nodes or not and the switching between states as a function of the details of the Fermi surface have been reached by other authors [9,10].

Another complicating factor is the three-dimensional structure of the iron-pnictides. In the above, the Fermi surfaces have been assumed to be predominately two-dimensional. However, even for the 1111-compounds (such as LaFePO) which are the most two-dimensional [3] there is considerable warping along the c-direction, especially of the electron sheets. For the 122 compounds such as $BaFe_2(As_{1-x}P_x)_2$ there is considerable more warping [11]. In this case $\chi(\boldsymbol{q})$ will vary as a function for k_z which could lead to c-axis variation of Δ. For example, it has been proposed [12] that in $BaFe_2(As_{1-x}P_x)_2$ the gap nodes are localised to a highly warped section of one of the hole Fermi surface sheets, and that at other k_z values and on all the other Fermi surface sheets the gap is large.

1.2. Experimental probes of pairing states

Measurements of the temperature dependence of the magnetic penetration depth λ, which is the focus of this article, give important insights into the gap symmetry and anisotropy. Finite temperature causes low lying quasiparticle states to be populated and when a magnetic field is applied these quasiparticle states will generate a paramagnetic current which opposes the diamagnetic Meissner screening current and therefore increases λ. Hence, the temperature dependence of λ essentially probes the energy dependence of the density of state of the quasiparticle excitations $D(E)$. Although many other experimentally measurable quantities also probe $D(E)$ measurements of $\lambda(T)$ have many advantages. As the distance probed is of order a few thousand Angstroms, $\lambda(T)$ is a quasi-bulk probe. Although gross surface degradation will be important, $\lambda(T)$ measurements are considerably less sensitive to this and other surface related issues than for example tunnelling or photoemission spectroscopy which typically probe a few tens of Angstroms at most. Measurements of other bulk quantities, notably, thermal conductivity, specific heat and spin susceptibility via nuclear magnetic resonance (NMR) provide important additional information on the pairing state, and only when all these measurements are understood can definite conclusions be drawn.

1.3. Magnetic penetration depth

In the clean-limit, local, BCS theory the temperature dependence of the penetration depth is given by [13]

$$\lambda_x^{-2}(T) = \lambda_x^{-2}(0) + \frac{\mu_0 e^2}{4\pi^3\hbar} \oint \mathrm{d}S \frac{v_x^2}{|v_F|} \int_{\Delta_k}^{\infty} \mathrm{d}\varepsilon_k \left(-\frac{\partial f(\varepsilon_k)}{\varepsilon_k} \right) \frac{\varepsilon_k}{\sqrt{\varepsilon_k^2 - \Delta_k^2}} \tag{2}$$

where

$$\lambda_x^{-2}(0) = \frac{\mu_0 e^2}{4\pi^3\hbar} \oint \mathrm{d}S \frac{v_x^2}{|v_F|}$$

and f is the usual Fermi function, $\oint \mathrm{d}S$ refers to an integral over the whole Fermi surface, and v_x is the x-component of the Fermi velocity v_F. This is the expression for the component of λ which relates to currents flowing in the x-direction. Note that in this limit $\lambda(0)$ is a normal state property (in the Drude model $\lambda^{-2}(0) \propto n/m$) as the superconducting gap does not enter the expression. The local limit ($\lambda > \xi$, where ξ is the coherence length) is usually easily met except close to a node where ξ, which is proportional to Δ^{-1}, will diverge. Non-local effects can become important at very low temperature in nodal superconductors [14]. The reference to BCS theory here does not refer to a particular pairing mechanism

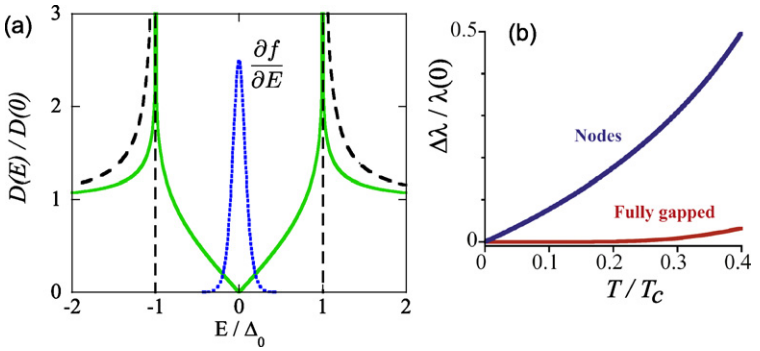

Fig. 2. (a) Quasiparticle density of states for an s (dashed line), $d_{x^2-y^2}$ gap function (solid line, Fermi surface averaged) in a quasi-two-dimensional metal (cuprate), along with the derivative of the Fermi function showing how finite temperature leads to the excitation of quasiparticles which produce a paramagnetic current and hence increase the penetration depth λ when a field is applied. (b) Temperature dependence of λ for fully gapped and nodal ($d_{x^2-y^2}$) pairing states.

but rather to the fact that the excitations from the superconducting ground state are assumed to be fermionic Bogolubov quasiparticles, rather than pair excitations (phase fluctuations) which would be the case if the superconductor was in the Bose–Einstein limit of local condensing pairs. The crossover between these limits should occur roughly when the coherence length becomes of order the lattice spacing. Pair excitations will further deplete the condensate and add to the temperature dependence of λ. It has been suggested that these could be important in underdoped cuprate and organic superconductors [15–18].

In the approximation that the Fermi velocity is constant, the expression for the temperature dependence of the superfluid density normalised to its zero temperature value may be simplified to

$$\tilde{\rho} = \frac{\lambda^2(0)}{\lambda^2(T)} = 1 + 2\int_0^\infty \mathrm{d}E \frac{\partial f(E)}{\partial E} \frac{\bar{D}(E)}{D(0)} \tag{3}$$

where E is the quasiparticle energy ($E^2 = \varepsilon^2 + \Delta^2$) and $\bar{D}(E)/D(0)$ is the angle averaged superconducting density of states divided by the normal state value at the Fermi level. The temperature dependence of λ is caused by a paramagnetic current carried by excited fermionic quasiparticles which partially cancels the screening current from the condensate. For the simple case of conventional superconductors where the Δ is constant for all points in k-space then for $k_B T \ll \Delta_0$, $\lambda(T)$ varies exponentially according to

$$\frac{\Delta\lambda(T)}{\lambda(0)} = \sqrt{\frac{\pi\Delta_0}{2k_B T}}\, e^{-\Delta_0/k_B T}. \tag{4}$$

Besides minor differences in prefactors ($\sim 10\%$) the above expression agrees well with the exact numerical solution to Eq. (2) up to $\sim T_c/3$. If the gap is finite everywhere but has different values on different Fermi surface sheets or is anisotropic on a particular sheet, then the above exponential behaviour will still be found when the temperature is much less than the minimum gap. So generally, if $\lambda(T)$ is essentially temperature independent at low temperature then this should indicate that there is a large finite gap at all points in k-space. However, if there is a rapid increase of penetration depth with increasing temperature this is indicative of a small value of the gap somewhere on the Fermi surface.

For the case of two-dimensional line nodes (e.g., the d-wave gap such as that found for cuprate superconductors: $\Delta(\phi) = \Delta_0 \cos 2\phi$, where ϕ is the in-plane azimuthal angle) the angle averaged density of states $\bar{D}(E) \propto E$ at low energy. This leads to $\Delta\lambda(T) = \lambda(T) - \lambda(0) \propto T$. More generally, the gap may have a more complicated form involving higher harmonics and so a useful parameterisation is the so-called triangular gap model [19] where it is assumed that Δ varies around the Fermi surface according to $\Delta(\phi) = \min(\mu\Delta_0\phi, \Delta_0)$, where $\mu\Delta_0 = 1/\mathrm{d}\Delta/\mathrm{d}\phi|_{\mathrm{node}}$ is the slope of the gap near the node. With $\mu = 2$ this produces a very similar form of $\lambda(T/T_c)$ to the more usual d-wave form $\Delta(\phi) = \Delta_0 \cos(2\phi)$. At low temperature $T \ll T_c$, this model predicts

$$\frac{\lambda^2(0)}{\lambda^2(T)} \simeq 1 - \frac{4\ln 2T}{\mu\Delta_0}. \tag{5}$$

So the slope of $\lambda^2(0)\lambda^2(T)$ with respect to temperature is proportional to the opening angle of the gap with respect to ϕ close to the node. Looking again at Eq. (2) it can be seen that in general the position of the nodes on the Fermi surface can make the temperature dependence of the different directional components of λ different. So for example, for a 2D orthorhombic material with a rectangular Fermi surface cross-section, if the nodes appear only on the edge of the rectangle parallel to x, then $\lambda_y(T)$ would show nodal behaviour but $\lambda_x(T)$ would appear fully gapped.

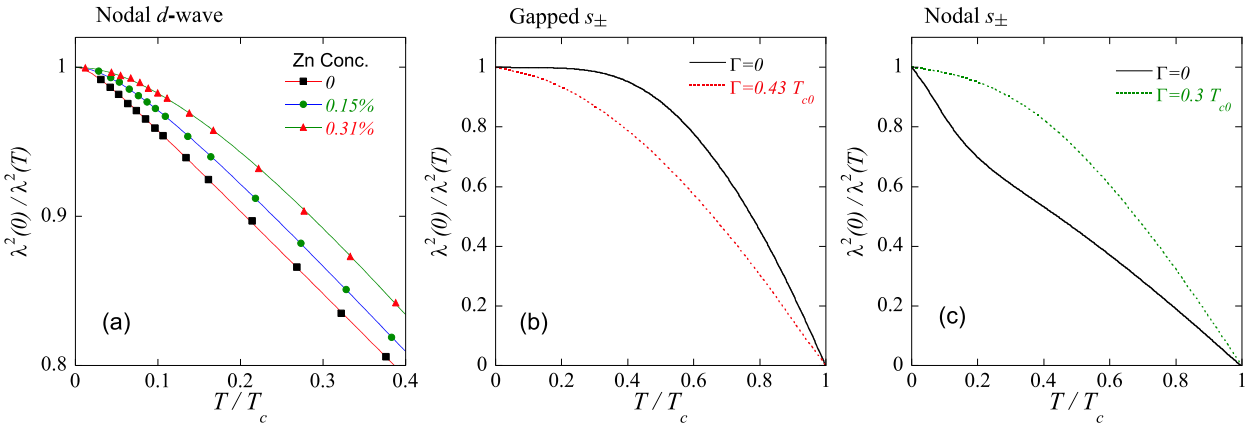

Fig. 3. Effect of impurity scattering on penetration depth for various pairing states. (a) shows data for pure and Zn-doped $YBa_2Cu_3O_{6.95}$ along with fits to Eq. (6) and is representative of the behaviour of a nodal $d_{x^2-y^2}$ gap symmetry with small amounts of disorder (adapted from Bonn et al. [26]). (b) shows a calculation for the fully gapped $s_\pm$ state. Γ is the scattering rate measured in units of the transition temperature of the pure material. The pure behaviour is exponential but evolves into a higher power law (with exponent ~ 2) as impurities are added (adapted from Vorontsov et al. [27]). (c) shows a calculation for a nodal $s_\pm$ state. The pure behaviour is linear in temperature but evolves into a higher power law (and eventually exponential) as impurities are added (adapted from Mishra et al. [28]).

In materials with multiple Fermi surface sheets the gap could have different magnitude or even different anisotropy on each sheet, i.e., some sheets could be fully gapped whereas others have nodes. Examples of such gap function for the iron-pnictides were discussed above. The integral over the Fermi surface in Eq. (2) can be split so that the integral is done on each Fermi surface sheet separately, and then the contributions added together. Furthermore, the gap on each sheet does not necessarily take the BCS weak coupling value. A common approach to dealing with this is the so-called alpha model [20,21]. Here the BCS weak-coupling form of $\Delta(T)$ is assumed but is multiplied by a temperature independent constant (alpha) to model the effect of the differing gap values. This approach works approximately because often $\lambda(T)$ depends more strongly on the magnitude of Δ rather than its precise temperature dependence. Self-consistent schemes [22] for calculating the temperature dependence of multiple interacting gaps have been developed but are more difficult to implement and often do not give significantly different results to fits using the weak-coupling forms of $\Delta(T)$ [23]. The major difference is only found very close to T_c where there is anyway more experimental uncertainty because of sample inhomogeneity.

1.4. Scattering

The above discussion of the interpretation of $\lambda(T)$ data does not take any account of impurity effects. Unfortunately, impurities are always present in crystals, and in doped iron-based superconductors their influence can be so strong that they mask the intrinsic behaviour. In a simple classical material with the gap having the same sign on all parts of the Fermi surface, scattering will simply average out the gap. Roughly, if there is an intrinsic variation of the gap on the Fermi surface of magnitude $\delta\Delta$ then this will be averaged to a uniform level if $\hbar\tau^{-1} > \sqrt{\delta\Delta\,\Delta_0}$ where τ^{-1} is the scattering rate and Δ_0 is the average gap [24]. If there is a sign changing gap the situation is more complicated. In single band cuprate superconductors, scattering will produce a small region close to the sign-changing node where there are broken-pair quasiparticles even at zero temperature, hence initially increasing the temperature from zero will have less of an effect than in the clean-limit. $\lambda(T)$ will change from its linear-in-temperature behaviour to a quadratic (T^2) behaviour as the temperature is reduced to below the impurity scattering energy. This cross-over is often modelled using the interpolation formula [25]

$$\Delta\lambda(T) = \frac{aT^2}{T + T^*} \tag{6}$$

where T^* parameterises the strength of the scattering and is related to the impurity scattering rate τ^{-1} [25].

Intra-band impurity scattering for the $s_\pm$ gap function proposed for the iron-pnictides has a similar effect. Namely, it produces a term in $\lambda(T)$ which varies like T^n with n varying according to the strength of the scattering from ~ 1.2 to ~ 2 [27]. So although there is a clear difference in the clean limit behaviour for $\lambda(T)$ for a nodal (e.g., d-wave) gap function or a fully gapped $s_\pm$ gap function when impurities are added the behaviour becomes rather similar. In both cases, $\lambda(T) \sim T^n$ with n close to 2. So therefore the observation of a power law dependence of $\lambda(T)$ with $n \sim 2$ could be consistent either with intrinsic nodal or fully gapped $s_\pm$ state with impurities. On the other hand, if $\lambda(T) \sim T$ (i.e., $n \simeq 1$) then this can only be explained by the presence of gap nodes in the clean-limit.

In the case that there is strong scattering, measurements of the thermal conductivity κ can be very helpful in determining the pairing state. If there are sign changing gap nodes on one or more Fermi surface sheet then it is expected that κ/T will have a finite limiting value as T approaches zero (the size of which depends on $\mu\Delta_0$ as for the slope of $\lambda(T)$ but

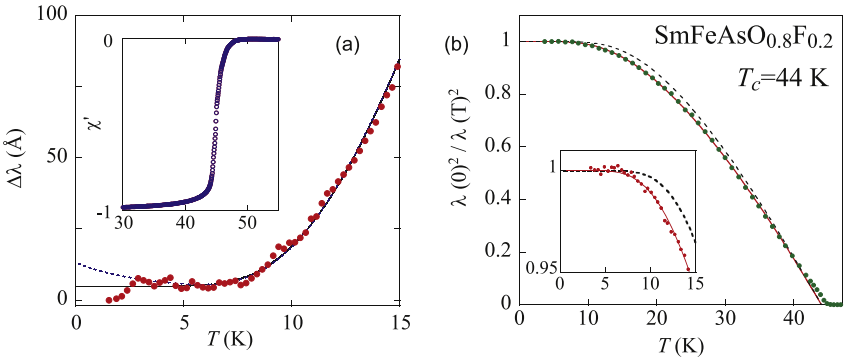

Fig. 4. (a) Low temperature behaviour of the in-plane penetration depth of $SmFeAsO_{0.8}F_{0.2}$. The solid line is a fit to the simple exponential relation Eq. (4) and the dashed line includes the effect of normal state paramagnetism, Eq. (7). (b) The calculated superfluid density for $SmFeAsO_{0.8}F_{0.2}$ assuming $\lambda(0) = 2600$ Å. The solid line is a fit to the two gap models ($\Delta_1 = 1.1k_BT_c$, $\Delta_2 = 1.7k_BT_c$) and the dashed line is the simple isotropic BCS behaviour (with $\Delta = 1.76T_c$). The inset shows an expanded view of the low temperature behaviour (after Malone et al. [33]).

crucially not on the amount of impurities [29,30]). Further, the field dependence of $\kappa(T)$ is very different for the nodal and gapped state. So this provides a useful tool to distinguish the two cases. Theory for the field and temperature dependence of κ for pairing states specific to the iron-based materials can be found in Ref. [31]. Finally, one possible gap-function for the iron-pnictides has non-sign changing gap nodes. Such nodes (sometimes termed *accidental* nodes) are lifted by impurity scattering as in the case of a simple *s*-wave superconductor with slight gap anisotropy, and hence the material which in the clean-limit has gap nodes will become fully gapped as impurities are added [28]. The behaviour will therefore be somewhat opposite to the fully gapped $s_\pm$ case, i.e., in the clean-limit $\lambda(T) \sim T$ but as dirt is added $\lambda(T) \sim T^2$ and eventually $\lambda(T) \sim \exp(\Delta/k_BT)$. The three different behaviours are illustrated in Fig. 3.

2. Experimental results

This section will review some of the experimental penetration depth data on the iron-based superconductors, concentrating on data which has been obtained by the Bristol group in collaboration with colleagues in other institutions. The results will be put into a broader context with discussion of results on related materials and other techniques by different groups.

Given the anisotropic nature of $\lambda(T)$ and more importantly the necessity to have undamaged pristine surfaces (on the length scale of λ), it is important to make measurements on high quality single crystal samples. These are often very small and so high sensitivity apparatus is needed to measure the small changes in $\lambda(T)$. The data described here were all taken using a radio frequency inductive method, where the superconducting shielding volume (and hence penetration depth) is determined by measuring the self-inductance of a copper coil into which the sample is placed. The coil forms part of a tank circuit which is driven by a tunnel diode at low temperature and at a frequency between 12 and 15 MHz. The probe field is very small (~ 1 μT) so contributions from vortices are minimal and in all cases discussed here was directed parallel to *c*, so that only in-plane currents were excited and the results reflect the behaviour of the in-plane penetration depth. The apparatus [32] is described in more detail in papers detailed below.

2.1. 1111-materials: $SmFeAsO_{1-x}F_y$

The 1111-compound $SmFeAsO_{1-x}F_y$ is of special importance because when optimally doped this has the highest $T_c = 55$ K of any iron-pnictide [34] discovered to date. Indeed, it was the discovery of this which first drew many researchers into the field as many thought that this heralded the imminent discovery of materials within this series with far higher T_c. So far this has not happened, but attention has nevertheless been sustained by the many other fascinating properties of these compounds, such as the similarities with the cuprates and that the pairing is likely not driven by conventional electron–phonon coupling.

Small plate-like single crystals with nominal composition $SmFeAsO_{0.8}F_{0.2}$ were used for this study with typical dimensions $(80 \times 80 \times 20)$ μm^3 (the smallest dimension was along the *c*-axis). The size of these samples are at the limit of the Bristol apparatus so the signal-to-noise level is lower than that normally achieved. The samples have a sharp superconducting transition with a $T_c \simeq 44$ K (see Fig. 4). Hence the samples are slightly off optimal doping but are nevertheless the sharp transition suggests that they are very homogeneous.

The results at low temperature show that below $T \simeq 7$ K $\lambda(T)$ tends to a constant value (Fig. 4), which suggests that there is a sizeable gap on all the parts of the Fermi surface. However, at $T = 3.2$ K there is a sharp downturn in the data which is likely to be due to the antiferromagnetic ordering of the Sm ion moments [35,36]. The solid line in Fig. 4 is a fit of the data to Eq. (4) between $T = 3.2$ K and 15 K. The lower temperature limit was chosen to avoid the influence of the Sm ion ordering transition. The gap value was found to be 58 ± 3 K, with very similar values found in two other samples.

This gap value gives $\Delta_0/k_BT_c = 1.1 \pm 0.1$, which is significantly lower than the weak-coupling s-wave BCS value of 1.76, and suggests the possibility of significant gap anisotropy or multiple gaps such as is found in, for example, $NbSe_2$ [37] and MgB_2 [38]. The effect of a second (or multiple) gap is best appreciated by analysing the temperature dependence of the normalised superfluid density which is related the measured $\Delta\lambda(T)$ by $\tilde{\rho} = [\lambda(0)/(\lambda(0) + \Delta\lambda(T))^2]$. As the value of $\lambda(0)$ is not easily accessible in susceptibility measurements like those described here, this value is estimated from other experiments, for example μSR. Also because of surface roughness the effective values of $\lambda(0)$ are usually higher than the bulk values. In Fig. 4 $\tilde{\rho}$ is shown with a representative value of $\lambda(0) = 2600$ Å. Different values of $\lambda(0)$ within $\pm$ 20% have only a minor quantitative effect on the result. The dashed line in the figure shows the isotropic s-wave BCS prediction with $\Delta_0 = 1.76k_BT_c$. Although this is an acceptable fit to the higher temperature data it fails to account for the lowest temperature data because the gap is too large (as shown by the low temperature exponential fits described above). However, a two gap fit, where both gaps are assumed to be isotropic s-wave gaps, agrees with the data very well over most of the temperature range, except very close to T_c where inhomogeneity and fluctuation effects become important. The value of the larger gap is determined to be $\Delta_2/k_BT_c = 1.7 \pm 0.2$ which accounts for 80 ± 5% of the superfluid density. It should be noted that in cases where the two gaps are not very different it is difficult to experimentally differentiate between models where the gap is different on separate Fermi surface sheets (i.e., the above two gap model) and where the gap various continuously on all sheets [37]. Controlled studies of the influence of impurities on T_c and $\lambda(T)$ are very useful in this regard.

The apparent ordering of the Sm ions at 3.2 K highlights the effect of magnetism on the behaviour of the penetration depth. If the normal state is paramagnetic the susceptibility enters the analysis both as a result of modifying the solution of London's equation so that the field penetrates a shorter distance into the conductor and also gives a paramagnetic contribution from the region of the sample where the field has penetrated [39]. The end result is that the apparent measured penetration depth λ_m is related to the London depth λ_L (for example as given by Eq. (2)) by $\lambda_m(T) = \lambda_L(T)\sqrt{1 + \chi_N(T)}$ where $\chi_N(T)$ is the normal state susceptibility [39]. Assuming a simple Curie law form for $\chi_N(T)$ then for $\chi_N(T) \ll 1$ the additional contribution to the measured penetration depth due to the normal state paramagnetism is given by

$$\Delta\lambda_{\mathrm{NP}} = \frac{n_i\lambda_L(0)\mu_0\mu_e^2}{6k_BV_{\mathrm{cell}}T} \tag{7}$$

where n_i is the number of magnetic ions per unit cell, V_{cell} is the unit cell volume and μ_e is the effective magnetic moment of the paramagnetic ion. In cuprate superconductors, Cooper showed that this correction changed the apparent almost flat low temperature behaviour of λ_m in $Nd_{1.85}Ce_{0.15}CuO_{4-y}$ to an approximate T^2 power law, thus showing that the data were consistent with a d-wave gap anisotropy (in the dirty limit) rather than a fully gapped state as was previous thought. However, applying this analysis to the Sm-1111 case does not make a significant difference to the results, basically because the expected normal state magnetism is too weak at the minimum temperature. It is not possible to fit the data with a power-law temperature exponent of less than around 3 with realistic value of the Curie constant. Although, of course, having to make assumptions about the normal state magnetism does give some ambiguity to the result.

Penetration depth data for $PrFeAsO_{1-y}$ ($T_c = 35$ K) [40] also show evidence for fully gapped behaviour similar to that reported here. Again, to fit the full temperature dependence of $\tilde{\rho}$ a two gap model was required. For this compound there was no evidence of rare earth ion ordering. However, for Nd-1111 member of this series a strong upturn in λ_m was observed at low temperature consistent with the magnetic contributions discussed above [41]. After subtracting this magnetic contribution fits suggested that a T^2 power law described the data better. Data for La-1111 also showed a T^2 behaviour this time without a low T upturn [41].

2.2. Disordered materials: $FeTe_{0.5}Se_{0.5}$ and Co/K-doped Ba-122

The iron-chalcogenide compounds $FeTe_xSe_y$ share many properties with their iron-pnictide counterparts. Both families have Fermi surfaces composed of similar quasi-two-dimensional electron and hole pockets [43,44] and so if this unusual Fermi surface topology is the origin of the superconductivity and other unusual properties then many similarities should be expected between them. Conversely, the differences could highlight what are the most important parameters for high T_c superconductivity. The iron-chalcogenides have the benefit of having a much simpler structure than their iron-pnictide counterparts because there are no guest ions or interleaved layers separating the iron-chalcogenide layers. Although FeSe has a T_c up to 37 K under pressure [45–47], at ambient pressure the composition $FeTe_{0.5}Se_{0.5}$ seems to have this highest T_c ($\sim$14 K) [48].

The low temperature behaviour of $\Delta\lambda(T)$ is shown in Fig. 5. There is no evidence of any saturation and below $T \simeq 0.5$ K there is a small upturn in $\Delta\lambda(T)$. As described above, this upturn almost certainly results from normal state paramagnetism and so the data are fitted to a $\Delta\lambda(T) = AT^n + \frac{\mathcal{C}}{T} + \lambda_{\mathrm{offset}}$. This equation fits the data very well, with $n = 2.2 \pm 0.1$, $\mathcal{C} = 1.24$ Å/K. This value of $\mathcal{C}$ corresponds to an average moment of $0.16\mu_B$ per unit cell (assuming $\lambda_L(0) = 5000$ Å) [49]. This small moment could come from the bulk Fe atoms or possibly from a small amount of free Fe impurities (although none were detected in X-ray measurements of this sample [42]).

The observed power law exponent is close to 2 which could indicate either a nodal state in the presence of disorder or instead could result from strong interband scattering between two intrinsically fully gapped Fermi surface sheets with sign changing gap between the sheets (i.e., the fully gapped $s_\pm$ state). This behaviour is typical of highly disordered iron-based superconductors. In particular, very similar behaviour is found for the Co-doped Ba-122 series [50,51], $Ba(Fe_{1-x}Co_x)_2As_2$,

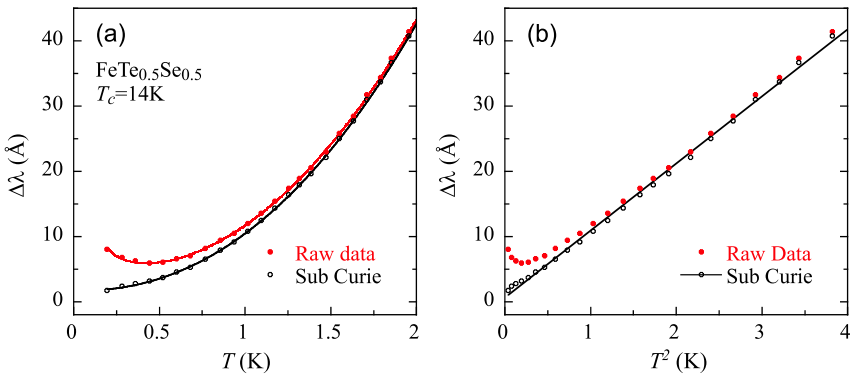

Fig. 5. (a) Low temperature behaviour of in-plane penetration depth of single crystal $FeTe_{0.5}Se_{0.5}$. The solid symbols are the raw data and solid line is a fit including a Curie-like normal state paramagnetic term. The open symbol shows the data with this Curie term subtracted and the fit is then just to a power law $\Delta\lambda = AT^n + B$. (b) The same data plotted against T^2 along with a straight line fit (after Serafin et al. [42]).

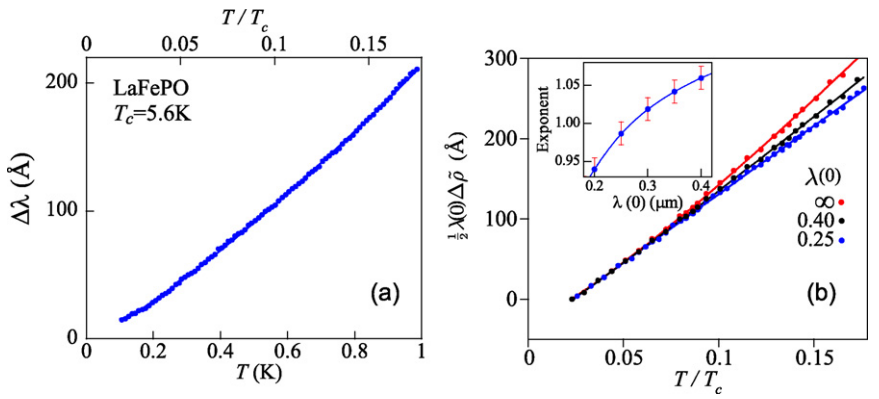

Fig. 6. (a) Low temperature in-plane penetration depth of single crystal LaFePO. (b) Same data plotted as normalised superfluid density, with difference choices for $\lambda(0)$ as indicated along with a fit to a power-law. The normalisation factor is chosen so that for $\lambda(0) = \infty$ the quantity plotted, $\frac{1}{2}\lambda(0)[1 - \lambda^2(0)/\{\lambda(0) + \Delta\lambda(T)\}^2]$, exactly equals the raw data $\Delta\lambda(T)$. The inset shows the dependence of the power-law exponent on the choice of $\lambda(0)$ (after Fletcher et al. [58]).

where the dopant substitutes directly into the Fe plane which is responsible for the conduction in the normal and superconducting states. The results for K-doped Ba-122 are controversial. Martin et al. [52] conclude that a T^2 power law is obeyed however, Hashimoto et al. [53] show that $\Delta\lambda(T)$ depends very strongly on the disorder in the sample ($Ba_{1-x}K_xFe_2As_2$ is highly air sensitive so must be protected from contact with air), and tends towards an exponential dependence for their best sample. This and the observed dependence of $\lambda(T)$ on induced irradiation damage [54] in $Ba(Fe_{1-x}Co_x)_2As_2$ is exactly the behaviour expected if the pairing state is intrinsically fully gapped $s_\pm$ but is strongly disordered. This view is also supported by the thermal conductivity measurements. In Co- and K-doped Ba-122 [55,56] as well as $FeSe_x$ [57] measurements suggest that the value of κ/T extrapolated to a very small value at $T = 0$ (compared to the normal state value) and hence indicates the absence of sign-changing gap nodes in these materials [31].

2.3. Low disorder/low T_c: LaFePO, KFe_2As_2

The iron phosphide superconductor LaFePO was actually the first iron-pnictide superconductor discovered in 2006 [59]. However, at that time it received only limited attention because it has a relatively low $T_c \sim 6$ K. It is isomorphic with LaFeAsO (La-1111) and it was the discovery of high T_c superconductivity [60] (especially under pressure, T_c up to 43 K) [61] in this latter compound which sparked the iron-pnictide field. The relatively low T_c of LaFePO has been linked to the fact that the Fe–P bond angles depart substantially from those of a regular tetrahedron [62]. Unlike the corresponding As-based compound, nominally undoped LaFePO is non-magnetic and superconducting [63], and crucially it is very clean with mean-free paths of order 1000 Å [3]. Its Fermi surface has been accurately determined by de Haas–van Alphen measurements [3] and is found to be in close agreement with conventional band-structure calculations with a modest renormalisation (factor 2) of the quasiparticle masses. Its Fermi surface is almost identical to that predicted for LaFeAsO.

The low temperature in-plane penetration depth data, shown in Fig. 6 is approximately linear with T which is strongly indicative of nodes in the order parameter. A variable power law fit, i.e. $\Delta\lambda(T) \propto T^n$ for $T < 1$ K gives $n = 1.2 \pm 0.1$. For a nodal gap structure the normalised superfluid density $\tilde{\rho} = [\lambda(0)/\lambda(T)]^2$ varies linearly over a much wider range of T

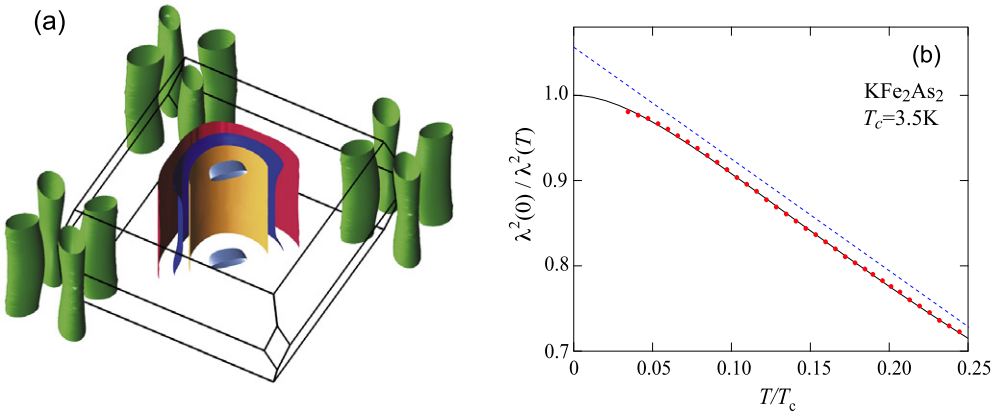

Fig. 7. (a) Fermi surface of KFe_2As_2 estimated from fits to the dHvA data. (b) Low temperature behaviour of the in-plane superfluid density of single crystal KFe_2As_2 (after Hashimoto et al. [71]).

than $\lambda(T)$ however, it is not trivial to estimate $\lambda(0)$ for LaFePO because at present there is no single crystal μSR data. Measurements of polycrystalline samples [64] suggest $\lambda(0) \simeq 2400$ Å, however, μSR data for λ needs to be viewed with some caution in cases where a well formed flux lattice has not been demonstrated [65]. Given this uncertainty and that in the calibration factor relating the observed oscillator frequency shift to $\Delta\lambda(T)$ it is useful to see how the variation in the assumed value of $\lambda(0)$ affects the calculated temperature dependence of $\tilde{\rho}$. In Fig. 6 the temperature dependent part of the superfluid density ($\Delta\tilde{\rho} = 1 - \tilde{\rho}$) multiplied by a scale factor $\lambda(0)/2$ is plotted. For $\lambda(0) = \infty$ this is exactly equal to $\Delta\lambda(T)$ and so the figure shows directly how different assumed values of $\lambda(0)$ effect the temperature dependence of the superfluid density. The range of $\lambda(0)$ values plotted encompasses our uncertainty in our calibration factors and also $\lambda(0)$. A fit of $\tilde{\rho}$ to a power law, shows that the exponent is equal to unity within an uncertainty of 5% with $\lambda(0)$ in the range 2000–4000 Å.

The importance of the observation of a linear T dependence of the superfluid density over a wide range of temperature is that it is very difficult to produce this from extrinsic effects. Magnetism, and impurities both cause the T dependence of λ to weaken. Although power-laws (with $n \sim 2$) point towards an unconventional gap symmetry they can be produced either with or without nodes. However, the linear dependence observed here strongly points towards nodes. This is further supported both by independent measurements of $\lambda(T)$ using a miniature SQUID magnetometer [66], and also measurement of thermal conductivity [67]. For LaFePO, κ/T has a large residual value at low T.

One point which is worth further discussion is that it has been suggested [68] that perfectly stoichiometric LaFePO is not superconducting and is only superconducting if there is an oxygen deficiency or if it is doped with F. If this is correct it could be that samples may have macroscopically separated regions of superconducting and non-superconducting material. Proximity coupling between these components can give a strong T dependence to λ over a limited temperature interval, but invariably there will be a strong down turn as the normal metal part becomes fully superconducting [69]. For LaFePO there was no sign of such a downturn in any of the samples measured and indeed in the best samples the SQUID microscopy showed that the screening was very homogeneous [66].

Another very clean iron-based superconductor is KFe_2As_2. The sample used for the penetration depth study had residual resistance ratios of more than 1000, and again dHvA oscillations could be used to map out the Fermi surface [70]. This material can be viewed as the end member of the $Ba_{1-x}K_xFe_2As_2$ and has a low $T_c \sim 3$ K. The material is very air sensitive so samples were enveloped in grease when handled in air. Unlike other iron-based superconductors the Fermi surface does not have the characteristic electron and hole pockets. Compared to $BaFe_2As_2$ it has one extra hole per unit cell, this leads to the crossing of an extra band near the M-point and the electron pockets transform in to small hole cylinders. In Fig. 7 an estimate of the Fermi surface topology based on best fits of the band-structure to the dHvA data is shown.

The penetration depth data, like LaFePO, show a strong linear behaviour, again consistent with line nodes. The superfluid density calculated with an estimated [71] value of $\lambda(0)$ is shown in Fig. 7. At the lowest temperatures $T/T_c \lesssim 0.07$ $\lambda(T)$ begins to flatten which is consistent with a small amount of impurity scattering. The size of the slope of $\tilde{\rho}(T)$ shows that the reduction in superfluid density is occurring over a large portion of the Fermi surface. This mean that there must be either horizontal or vertical line nodes on one or more of the zone centre hole sheets. The conclusion that there are line nodes in this material is also supported by NQR [72], specific-heat [72], thermal conductivity [73] measurements as well as measurements of $\lambda(T)$ using small angle neutron scattering [74].

2.4. Low disorder/ high T_c: $BaFe_2(As_{1-x}P_x)_2$

From the above account of the differences in behaviour of $\lambda(T)$ between the higher T_c 1111-compounds, Co/K-doped Ba-122/FeSeTe and the low T_c materials LaFePO and KFe_2As_2, it is natural to question whether the nodal behaviour is a consequence or cause of their low T_c. That is to say, is the nodal state in LaFePO because the higher T_c nodeless pairing channel is not operative in this material? Insight into this question can be found in studies of the P-doped Ba-122 system

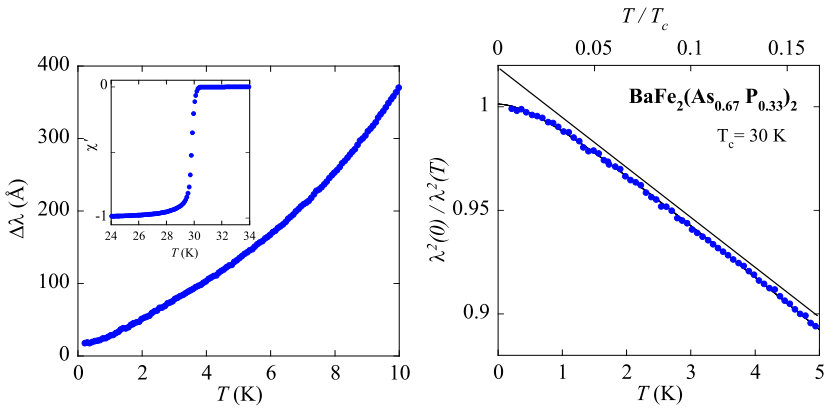

Fig. 8. (a) Low temperature in-plane penetration depth of single crystal $BaFe_2(As_{0.67}P_{0.33})_2$. The inset shows the susceptibility close to the transition. (b) The superfluid density. In this experiment $\lambda(0)$ was measured directly using microwave measurements. The solid line going through the data is a fit to Eq. (6). The other line emphasises the linear behaviour (after Hashimoto et al. [75]).

$BaFe_2(As_{1-x}P_x)_2$. Here P is an isovalent substitution for As, so there is no charge doping involved. The P substitution does however cause a substantial reduction in the lattice c/a ratio and hence its main effect is applying chemical pressure. The end member $BaFe_2As_2$ a spin-density-wave itinerant antiferromagnet, and doping it with P causes the ordering temperature to fall, and the material first becomes superconducting at $x \simeq 0.16$ [76]. The T_c is maximum at $x = 0.33$ and then at $x = 0.7$ T_c is again zero and the ground state is a paramagnetic metal. Importantly, the isovalent As/P substitution seems to produce considerable less disorder on the conducting Fe plane than other charged dopants (K/Co) so that the residual resistance remains low [76] and quantum oscillations are observable up to at least $x = 0.41$ ($T_c = 25$ K) [11].

The in-plane penetration depth data for single crystal $BaFe_2(As_{0.67}P_{0.33})_2$ are shown in Fig. 8. The low temperature behaviour of $\Delta\lambda(T)$ is linear which is again indicative of nodes. At the lowest temperatures there is a flattening of the linear behaviour which in some samples turns into a small upturn at the lowest temperatures. This is probably due to paramagnetic impurities or intrinsic paramagnetism of the normal state but could also result from the presence of low energy Andreev bound states [77]. A fit using the dirty d-wave formula Eq. (6) gives $T^* = 1.3\ \text{K} = 0.04T_c$ which is a small value comparable to that found for good quality optimally doped $YBa_2Cu_3O_{6-\delta}$ [78,26].

There is strong corroboration of this result both from thermal conductivity [71] and NMR data [79] which both also give clear indications of a nodal sign-changing pairing state. So it would appear that for the Ba-122 structure there are pairing states with nodes [$BaFe_2(As_{0.67}P_{0.33})_2$] and without nodes [$Ba_{0.45}K_{0.55}Fe_2As_2$] [53] which have a similar T_c of $\sim$30 K. This is unusual (if not unique) because, as mentioned in the introduction, nodes reduce the number of electrons which can pair so generally a nodal state has a lower T_c than one without nodes. It has been suggested that this might be explained if the nodes occur on a sheet of Fermi surface which is not strongly involved in the pairing [12]. These calculations suggest that the nodes occur on the largest hole sheet of Fermi surface and occur only close to the top of the Brillouin zone. This however, has not yet been verified experimentally.

3. Conclusions

Investigations of the nature of pairing in the iron-based superconductors continue to be of considerable interest with much rapid progress being made both experimentally and theoretically. The experiments described above seem to point to at least two different pairing states being operative. In one class of materials, LaFePO, KFe_2As_2 and $BaFe_2(As_{1-x}P_x)_2$ there is clear evidence of line nodes, whereas in another, 1111-materials ($SmFeAsO_{1-x}F_y$), K- and Co-doped Ba-122, and $FeSe_xTe_y$ there do not appear to be any sign-changing nodes. The existence of nodes in $BaFe_2(As_{0.66}P_{0.33})_2$ clearly shows that nodes are not solely linked to low T_c materials. It may be co-incidental but it is worth remarking that so far all the nodal materials that have been discovered are much cleaner (longer mean-free-paths) than the nodeless ones. To what extent disorder plays a role in determining the gap structure is at the moment unclear. Theoretical treatments to date suggest it does not play any role, apart from obscuring the intrinsic behaviour in experimental quantities that probe the density of states (penetration depth, specific heat, NMR).

The picture that seems to be emerging is that the pairing interaction is driven by antiferromagnetic spin fluctuations and the multi-band nature of the Fermi surface leads to a number of competing pairing channels which are close in energy. In the majority of materials, five Fe d-bands cross the Fermi level (or are close to crossing it) and small differences in the energies of these bands can lead to significant changes in the Fermi surface topology. This in turn leads to changes in the frequency and momentum dependence of the spin-susceptibility which, in this model, affects the pairing. This scenario is however, still far from being verified. For example, it has recently been argued that the effect of impurities on the superconductivity is far less than that calculated from an $s_\pm$ type gap (with or without nodes) [80] and that paring may instead be mediated by orbital fluctuations [81] which leads to a non-sign changing s_{++} gap. Further experimental work on

looking at the systematics of variation of the pairing states across the various iron-based superconducting families and how these are effected by the addition of controlled amounts of impurities will help to answer these questions.

Acknowledgements

The experiments described in this review have been performed in collaboration with colleagues both in Bristol and other laboratories around the world. I would particularly like to acknowledge the contributions of Jon Fletcher, Liam Malone, Alessandro Serafin and Kenichiro Hashimoto who were involved with the measurements in Bristol and the groups of Ian Fisher and Jim Analytis (Stanford), Yuji Matsuda, Takasada Shibauchi, and Shigeru Kasahara (Kyoto), Hideto Fukazawa (Chiba), Janusz Karpinski (Zürich) and Alexey Ganin, Matthew Rosseinsky (Liverpool) for providing samples, scientific discussions and supporting measurements. Numerous other colleagues were also involved in the sample growth; here I merely list representatives from each team. This work was supported by the UK EPSRC.

References

[1] A.F. Bangura, P.M.C. Rourke, T.M. Benseman, M. Matusiak, J.R. Cooper, N.E. Hussey, A. Carrington, Fermi surface and electronic homogeneity of the overdoped cuprate superconductor $Tl_2Ba_2CuO_{6+\delta}$ as revealed by quantum oscillations, Phys. Rev. B 82 (14) (2010) 140501(R).
[2] P.M.C. Rourke, A.F. Bangura, T.M. Benseman, M. Matusiak, J.R. Cooper, A. Carrington, N.E. Hussey, A detailed de Haas–van Alphen effect study of the overdoped cuprate $Tl_2Ba_2CuO_{6+\delta}$, New J. Phys. 12 (10) (2010) 105009.
[3] A.I. Coldea, J.D. Fletcher, A. Carrington, J.G. Analytis, A.F. Bangura, J.-H. Chu, A.S. Erickson, I.R. Fisher, N.E. Hussey, R.D. McDonald, Fermi surface of superconducting LaFePO determined from quantum oscillations, Phys. Rev. Lett. 101 (21) (2008) 216402.
[4] M. Tinkham, Introduction to Superconductivity, 2nd edition, Dover Publications Inc., 2004.
[5] D.J. Scalapino, The case for $d_{x^2-y^2}$ pairing in the cuprate superconductors, Phys. Rep. 250 (1995) 329.
[6] I.I. Mazin, D.J. Singh, M.D. Johannes, M.H. Du, Unconventional sign-reversing superconductivity in $LaFeAsO_{1-x}F_x$, Phys. Rev. Lett. 101 (2008) 057003.
[7] K. Kuroki, S. Onari, R. Arita, H. Usui, Y. Tanaka, H. Kontani, H. Aoki, Unconventional pairing originating from the disconnected Fermi surfaces of superconducting $LaFeAsO_{1-x}F_x$, Phys. Rev. Lett. 101 (2008) 087004.
[8] S. Graser, T.A. Maier, P.J. Hirschfeld, D.J. Scalapino, Near-degeneracy of several pairing channels in multiorbital models for the Fe pnictides, New J. Phys. 11 (2009) 025016.
[9] A.V. Chubukov, M.G. Vavilov, A.B. Vorontsov, Momentum dependence and nodes of the superconducting gap in the iron pnictides, Phys. Rev. B 80 (2009) 140515.
[10] K. Kuroki, H. Usui, S. Onari, R. Arita, H. Aoki, Pnictogen height as a possible switch between high-T_c nodeless and low-T_c nodal pairings in the iron-based superconductors, Phys. Rev. B 79 (2009) 224511.
[11] H. Shishido, A.F. Bangura, A.I. Coldea, S. Tonegawa, K. Hashimoto, S. Kasahara, P.M.C. Rourke, H. Ikeda, T. Terashima, R. Settai, Y. Onuki, D. Vignolles, C. Proust, B. Vignolle, A. McCollam, Y. Matsuda, T. Shibauchi, A. Carrington, Evolution of the Fermi surface of $BaFe_2(As_{1-x}P_x)_2$ on entering the superconducting dome, Phys. Rev. Lett. 104 (2010) 057008.
[12] K. Suzuki, H. Usui, K. Kuroki, Possible three dimensional nodes in the $s\pm$ superconducting gap of $BaFe_2(As_{1-x}P_x)_2$, J. Phys. Soc. Jpn. 80 (2011) 013710.
[13] B.S. Chandrasekhar, D. Einzel, The superconducting penetration depth from the semiclassical model, Ann. Phys. (Leipzig) 2 (1993) 535–546.
[14] I. Kosztin, A.J. Leggett, Nonlocal effects on the magnetic penetration depth in d-wave superconductors, Phys. Rev. Lett. 79 (1) (1997) 135–138.
[15] I. Kosztin, Q. Chen, B. Jankó, K. Levin, Relationship between the pseudo- and superconducting gaps: Effects of residual pairing correlations below T_c, Phys. Rev. B 58 (10) (1998) R5936–R5939.
[16] Q. Chen, I. Kosztin, B. Jankó, K. Levin, Pairing fluctuation theory of superconducting properties in underdoped to overdoped cuprates, Phys. Rev. Lett. 81 (21) (1998) 4708–4711.
[17] Q. Chen, I. Kosztin, K. Levin, Unusual thermodynamical and transport signatures of the BCS to Bose–Einstein crossover scenario below T_c, Phys. Rev. Lett. 85 (13) (2000) 2801–2804.
[18] V. Emery, S. Kivelson, Importance of phase fluctuations in superconductors with small superfluid density, Nature 374 (2002) 434–437.
[19] D. Xu, S.K. Yip, J.A. Sauls, Nonlinear Meissner effect in unconventional superconductors, Phys. Rev. B 51 (22) (1995) 16233–16253.
[20] H. Padamsee, J. Neighbor, C. Shiffman, Quasiparticle phenomenology for thermodynamics of strong-coupling superconductors, J. Low Temp. Phys. 12 (1973) 387.
[21] F. Bouquet, Y. Wang, R.A. Fisher, D.G. Hinks, J.D. Jorgensen, A. Junod, N.E. Phillips, Phenomenological two-gap model for the specific heat of MgB_2, Europhys. Lett. 56 (6) (2001) 856.
[22] V.G. Kogan, C. Martin, R. Prozorov, Superfluid density and specific heat within a self-consistent scheme for a two-band superconductor, Phys. Rev. B 80 (1) (2009) 014507.
[23] A. Carrington, F. Manzano, Magnetic penetration depth of MgB_2, Physica C 385 (2003) 205–214.
[24] I.I. Mazin, O.K. Andersen, O. Jepsen, A.A. Golubov, O.V. Dolgov, J. Kortus, Comment on "first-principles calculation of the superconducting transition in MgB_2 within the anisotropic Eliashberg formalism", Phys. Rev. B 69 (2004) 056501.
[25] P.J. Hirschfeld, N. Goldenfeld, Effect of strong scattering on the low-temperature penetration depth of a d-wave superconductor, Phys. Rev. B 48 (1993) 4219–4222.
[26] D.A. Bonn, S. Kamal, K. Zhang, R. Liang, D.J. Baar, E. Klein, W.N. Hardy, Comparison of the influence of Ni and Zn impurities on the electromagnetic properties of $YBa_2Cu_3O_{6.95}$, Phys. Rev. B 50 (6) (1994) 4051–4063.
[27] A.B. Vorontsov, M.G. Vavilov, A.V. Chubukov, Superfluid density and penetration depth in the iron pnictides, Phys. Rev. B 79 (2009) 140507.
[28] V. Mishra, G. Boyd, S. Graser, T. Maier, P.J. Hirschfeld, D.J. Scalapino, Lifting of nodes by disorder in extended-*s*-state superconductors: Application to ferropnictides, Phys. Rev. B 79 (2009) 094512.
[29] P.A. Lee, Localized states in a d-wave superconductor, Phys. Rev. Lett. 71 (12) (1993) 1887–1890.
[30] M.J. Graf, S.-K. Yip, J.A. Sauls, D. Rainer, Electronic thermal conductivity and the Wiedemann–Franz law for unconventional superconductors, Phys. Rev. B 53 (22) (1996) 15147–15161.
[31] V. Mishra, A. Vorontsov, P.J. Hirschfeld, I. Vekhter, Theory of thermal conductivity in extended-*s* state superconductors: Application to ferropnictides, Phys. Rev. B 80 (22) (2009) 224525.
[32] A. Carrington, R.W. Giannetta, J.T. Kim, J. Giapintzakis, Absence of nonlinear Meissner effect in $YBa_2Cu_3O_{6.95}$, Phys. Rev. B 59 (1999) R14173.
[33] L. Malone, J.D. Fletcher, A. Serafin, A. Carrington, N.D. Zhigadlo, Z. Bukowski, S. Katrych, J. Karpinski, Magnetic penetration depth of single-crystalline $SmFeAsO_{1-x}F_y$, Phys. Rev. B 79 (2009) 140501(R).
[34] Z.A. Ren, W. Lu, J. Yang, W. Yi, X.L. Shen, Z.C. Li, G.C. Che, X.L. Dong, L.L. Sun, F. Zhou, Z.X. Zhao, Superconductivity at 55 K in iron-based F-doped layered quaternary compound $Sm[O_{1-x}F_x]FeAs$, Chin. Phys. Lett. 25 (2008) 2215–2216.

[35] A.J. Drew, F.L. Pratt, T. Lancaster, S.J. Blundell, P.J. Baker, R.H. Liu, G. Wu, X.H. Chen, I. Watanabe, V.K. Malik, A. Dubroka, K.W. Kim, M. Rossle, C. Bernhard, Coexistence of magnetic fluctuations and superconductivity in the pnictide high temperature superconductor $SmFeAsO_{1-x}F_x$ measured by muon spin rotation, Phys. Rev. Lett. 101 (9) (2008) 097010.

[36] R. Khasanov, H. Luetkens, A. Amato, H.-H. Klauss, Z.A. Ren, J. Yang, W. Lu, Z.-X. Zhao, Muon-spin rotation studies of $SmFeAsO_{0.85}$ and $NdFeAsO_{0.85}$ superconductors, Phys. Rev. B 78 (2008) 092506.

[37] J.D. Fletcher, A. Carrington, O.J. Taylor, S.M. Kazakov, J. Karpinski, Temperature-dependent anisotropy of the penetration depth and coherence length of MgB_2, Phys. Rev. Lett. 95 (2005) 097005.

[38] F. Manzano, A. Carrington, N.E. Hussey, S. Lee, A. Yamamoto, S. Tajima, Exponential temperature dependence of the penetration depth in single crystal MgB_2, Phys. Rev. Lett. 88 (2002) 047002.

[39] J.R. Cooper, Power-law dependence of the ab-plane penetration depth in $Nd_{1.85}Ce_{0.15}CuO_{4-y}$, Phys. Rev. B 54 (1996) R3753–R3755.

[40] K. Hashimoto, T. Shibauchi, T. Kato, K. Ikada, R. Okazaki, H. Shishido, M. Ishikado, H. Kito, A. Iyo, H. Eisaki, S. Shamoto, Y. Matsuda, Microwave penetration depth and quasiparticle conductivity in single crystal $PrFeAsO_{1-y}$: Evidence for fully gapped superconductivity, Phys. Rev. Lett. 102 (2009) 017002.

[41] C. Martin, M.E. Tillman, H. Kim, M.A. Tanatar, S.K. Kim, A. Kreyssig, R.T. Gordon, M.D. Vannette, S. Nandi, V.G. Kogan, S.L. Bud'ko, P.C. Canfield, A.I. Goldman, R. Prozorov, Nonexponential London penetration depth of FeAs-based superconducting $RFeAsO_{0.9}F_{0.1}$ (R = La, Nd) single crystals, Phys. Rev. Lett. 102 (24) (2009) 247002.

[42] A. Serafin, A.I. Coldea, A.Y. Ganin, M.J. Rosseinsky, K. Prassides, D. Vignolles, A. Carrington, Anisotropic fluctuations and quasiparticle excitations in $FeSe_{0.5}Te_{0.5}$, Phys. Rev. B 82 (2010) 104514.

[43] A. Subedi, L.J. Zhang, D.J. Singh, M.H. Du, Density functional study of FeS, FeSe, and FeTe: Electronic structure, magnetism, phonons, and superconductivity, Phys. Rev. B 78 (2008) 134514.

[44] A. Tamai, A.Y. Ganin, E. Rozbicki, J. Bacsa, W. Meevasana, P.D.C. King, M. Caffio, R. Schaub, S. Margadonna, K. Prassides, M.J. Rosseinsky, F. Baumberger, Strong electron correlations in the normal state of the iron-based $FeSe_{0.42}Te_{0.58}$ superconductor observed by angle-resolved photoemission spectroscopy, Phys. Rev. Lett. 104 (2010) 097002.

[45] Y. Mizuguchi, F. Tomioka, S. Tsuda, T. Yamaguchi, Y. Takano, Superconductivity at 27 K in tetragonal FeSe under high pressure, Appl. Phys. Lett. 93 (2008) 152505.

[46] S. Medvedev, T.M. Mcqueen, I.A. Troyan, T. Palasyuk, M.I. Eremets, R.J. Cava, S. Naghavi, F. Casper, V. Ksenofontov, G. Wortmann, C. Felser, Electronic and magnetic phase diagram of β-$Fe_{1.01}Se$ with superconductivity at 36.7 K under pressure, Nat. Mater. 8 (2009) 630–633.

[47] S. Margadonna, Y. Takabayashi, Y. Ohishi, Y. Mizuguchi, Y. Takano, T. Kagayama, T. Nakagawa, M. Takata, K. Prassides, Pressure evolution of the low-temperature crystal structure and bonding of the superconductor FeSe ($T_c = 37$ K), Phys. Rev. B 80 (2009) 064506.

[48] K.W. Yeh, T.W. Huang, Y.L. Huang, T.K. Chen, F.C. Hsu, P.M. Wu, Y.C. Lee, Y.Y. Chu, C.L. Chen, J.Y. Luo, D.C. Yan, M.K. Wu, Tellurium substitution effect on superconductivity of the alpha-phase iron selenide, EPL 84 (2008) 37002.

[49] P.K. Biswas, G. Balakrishnan, D.M. Paul, C.V. Tomy, M.R. Lees, A.D. Hillier, Muon-spin-spectroscopy study of the penetration depth of $FeSe_{0.5}Te_{0.5}$, Phys. Rev. B 81 (2010) 092510.

[50] R.T. Gordon, N. Ni, C. Martin, M.A. Tanatar, M.D. Vannette, H. Kim, G.D. Samolyuk, J. Schmalian, S. Nandi, A. Kreyssig, A.I. Goldman, J.Q. Yan, S.L. Bud'ko, P.C. Canfield, R. Prozorov, Unconventional London penetration depth in single-crystal $Ba(Fe_{0.93}Co_{0.07})_2As_2$ superconductors, Phys. Rev. Lett. 102 (12) (2009) 127004.

[51] R.T. Gordon, C. Martin, H. Kim, N. Ni, M.A. Tanatar, J. Schmalian, I.I. Mazin, S.L. Bud'ko, P.C. Canfield, R. Prozorov, London penetration depth in single crystals of $Ba(Fe_{1-x}Co_x)_2As_2$ spanning underdoped to overdoped compositions, Phys. Rev. B 79 (2009) 100506.

[52] C. Martin, R.T. Gordon, M.A. Tanatar, H. Kim, N. Ni, S.L. Bud'ko, P.C. Canfield, H. Luo, H.H. Wen, Z. Wang, A.B. Vorontsov, V.G. Kogan, R. Prozorov, Nonexponential London penetration depth of external magnetic fields in superconducting $Ba_{1-x}K_xFe_2As_2$ single crystals, Phys. Rev. B 80 (2) (2009) 020501.

[53] K. Hashimoto, T. Shibauchi, S. Kasahara, K. Ikada, S. Tonegawa, T. Kato, R. Okazaki, C.J. van der Beek, M. Konczykowski, H. Takeya, K. Hirata, T. Terashima, Y. Matsuda, Microwave surface-impedance measurements of the magnetic penetration depth in single crystal $Ba_{1-x}K_xFe_2As_2$ superconductors: Evidence for a disorder-dependent superfluid density, Phys. Rev. Lett. 102 (20) (2009) 207001.

[54] H. Kim, R.T. Gordon, M.A. Tanatar, J. Hua, U. Welp, W.K. Kwok, N. Ni, S.L. Bud'ko, P.C. Canfield, A.B. Vorontsov, R. Prozorov, London penetration depth in $Ba(Fe_{1-x}T_x)_2As_2$ (T = Co, Ni) superconductors irradiated with heavy ions, Phys. Rev. B 82 (6) (2010) 060518.

[55] X.G. Luo, M.A. Tanatar, J.-P. Reid, H. Shakeripour, N. Doiron-Leyraud, N. Ni, S.L. Bud'ko, P.C. Canfield, H. Luo, Z. Wang, H.-H. Wen, R. Prozorov, L. Taillefer, Quasiparticle heat transport in single-crystalline $Ba_{1-x}K_xFe_2As_2$: Evidence for a k-dependent superconducting gap without nodes, Phys. Rev. B 80 (2009) 140503.

[56] M.A. Tanatar, J.-P. Reid, H. Shakeripour, X.G. Luo, N. Doiron-Leyraud, N. Ni, S.L. Bud'ko, P.C. Canfield, R. Prozorov, L. Taillefer, Doping dependence of heat transport in the iron-arsenide superconductor $Ba(Fe_{1-x}Co_x)_2As_2$: From isotropic to a strongly k-dependent gap structure, Phys. Rev. Lett. 104 (6) (2010) 067002.

[57] J.K. Dong, T.Y. Guan, S.Y. Zhou, X. Qiu, L. Ding, C. Zhang, U. Patel, Z.L. Xiao, S.Y. Li, Multigap nodeless superconductivity in $FeSe_x$: Evidence from quasiparticle heat transport, Phys. Rev. B 80 (2009) 024518.

[58] J.D. Fletcher, A. Serafin, L. Malone, J.G. Analytis, J.-H. Chu, A.S. Erickson, I.R. Fisher, A. Carrington, Evidence for a nodal-line superconducting state in LaFePO, Phys. Rev. Lett. 102 (2009) 147001.

[59] Y. Kamihara, H. Hiramatsu, M. Hirano, R. Kawamura, H. Yanagi, T. Kamiya, H. Hosono, Iron-based layered superconductor: LaOFeP, J. Amer. Chem. Soc. 128 (31) (2006) 10012–10013.

[60] Y. Kamihara, T. Watanabe, M. Hirano, H. Hosono, Iron-based layered superconductor $La[O_{1-x}F_x]FeAs$ ($x = 0.05$–0.12) with $T_c = 26$ K, J. Amer. Chem. Soc. 130 (2008) 3296–3297.

[61] H. Takahashi, K. Igawa, K. Arii, Y. Kamihara, M. Hirano, H. Hosono, Superconductivity at 43 K in an iron-based layered compound $LaO_{1-x}F_xFeAs$, Nature 453 (2008) 376–378.

[62] C.-H. Lee, A. Iyo, H. Eisaki, H. Kito, M.T. Fernandez-Diaz, T. Ito, K. Kihou, H. Matsuhata, M. Braden, K. Yamada, Effect of structural parameters on superconductivity in fluorine-free $LnFeAsO_{1-y}$ (Ln = La, Nd), J. Phys. Soc. Jpn. 77 (2008) 083704.

[63] J.G. Analytis, J.-H. Chu, A. S. Erickson, C. Kucharczyk, A. Serafin, A. Carrington, C. Cox, S.M. Kauzlarich, H. Hope, I.R. Fisher, Bulk superconductivity and disorder in single crystals of LaFePO, arXiv:0810.5368 (unpublished).

[64] Y. Uemura, Energy-scale phenomenology and pairing via resonant spin-charge motion in FeAs, CuO, heavy-fermion and other exotic superconductors, Physica B 404 (19) (2009) 3195–3201.

[65] J. Sonier, W. Huang, C. Kaiser, C. Cochrane, V. Pacradouni, S. Sabok-Sayr, M. Lumsden, B. Sales, M. McGuire, A. Sefat, D. Mandrus, Magnetism and disorder effects on muSr measurements of the magnetic penetration depth in iron-based superconductors, Phys. Rev. Lett. 106 (2011) 127002.

[66] C.W. Hicks, T.M. Lippman, M.E. Huber, J.G. Analytis, J.-H. Chu, A.S. Erickson, I.R. Fisher, K.A. Moler, Evidence for a nodal energy gap in the iron-pnictide superconductor LaFePO from penetration depth measurements by scanning squid susceptometry, Phys. Rev. Lett. 103 (12) (2009) 127003.

[67] M. Yamashita, N. Nakata, Y. Senshu, S. Tonegawa, K. Ikada, K. Hashimoto, H. Sugawara, T. Shibauchi, Y. Matsuda, Thermal conductivity measurements of the energy-gap anisotropy of superconducting LaFePO at low temperatures, Phys. Rev. B 80 (2009) 220509.

[68] T.M. McQueen, M. Regulacio, A.J. Williams, Q. Huang, J.W. Lynn, Y.S. Hor, D.V. West, M.A. Green, R.J. Cava, Intrinsic properties of stoichiometric LaFePO, Phys. Rev. B 78 (2) (2008) 024521.
[69] R. Prozorov, R.W. Giannetta, S.L. Bud'ko, P.C. Canfield, Energy gap and proximity effect in MgB_2 superconducting wires, Phys. Rev. B 64 (2001) 180501.
[70] T. Terashima, M. Kimata, N. Kurita, H. Satsukawa, A. Harada, K. Hazama, M. Imai, A. Sato, K. Kihou, C.-H. Lee, H. Kito, H. Eisaki, A. Iyo, T. Saito, H. Fukazawa, Y. Kohori, H. Harima, S. Uji, Fermi surface and mass enhancement in KFe_2As_2 from de Haas–van Alphen effect measurements, J. Phys. Soc. Jpn. 79 (2010) 053702.
[71] K. Hashimoto, A. Serafin, S. Tonegawa, R. Katsumata, R. Okazaki, T. Saito, H. Fukazawa, Y. Kohori, K. Kihou, C.H. Lee, A. Iyo, H. Eisaki, H. Ikeda, Y. Matsuda, A. Carrington, T. Shibauchi, Evidence for superconducting gap nodes in the zone-centered hole bands of KFe_2As_2 from magnetic penetration-depth measurements, Phys. Rev. B 82 (2010) 014526.
[72] H. Fukazawa, Y. Yamada, K. Kondo, T. Saito, Y. Kohori, K. Kuga, Y. Matsumoto, S. Nakatsuji, H. Kito, P.M. Shirage, K. Kihou, N. Takeshita, C.-H. Lee, A. Iyo, H. Eisaki, Possible multiple gap superconductivity with line nodes in heavily hole-doped superconductor KFe_2As_2 studied by ^{75}As nuclear quadrupole resonance and specific heat, J. Phys. Soc. Jpn. 78 (2009) 083712.
[73] J.K. Dong, S.Y. Zhou, T.Y. Guan, H. Zhang, Y.F. Dai, X. Qiu, X.F. Wang, Y. He, X.H. Chen, S.Y. Li, Quantum criticality and nodal superconductivity in the FeAs-based superconductor KFe_2As_2, Phys. Rev. Lett. 104 (8) (2010) 087005.
[74] H. Kawano-Furukawa, C.J. Bowell, J.S. White, R. Heslop, A. Cameron, E. Forgan, K. Kihou, C.H. Lee, A. Iyo, H. Eisaki, T. Saito, H. Fukazawa, Y. Kohori, R. Cubitt, C.D. Dewhurst, J.L. Gavilano, M. Zolliker, The pairing state in KFe_2As_2 studied by measurements of the magnetic vortex lattice, arXiv:1005.4468.
[75] K. Hashimoto, M. Yamashita, S. Kasahara, Y. Senshu, N. Nakata, S. Tonegawa, K. Ikada, A. Serafin, A. Carrington, T. Terashima, H. Ikeda, T. Shibauchi, Y. Matsuda, Line nodes in the energy gap of superconducting $BaFe_2(As_{1-x}P_x)_2$ single crystals as seen via penetration depth and thermal conductivity, Phys. Rev. B 81 (2010) 220501(R).
[76] S. Kasahara, T. Shibauchi, K. Hashimoto, K. Ikada, S. Tonegawa, R. Okazaki, H. Shishido, H. Ikeda, H. Takeya, K. Hirata, T. Terashima, Y. Matsuda, Evolution from non-Fermi- to Fermi-liquid transport via isovalent doping in $BaFe_2(As_{1-x}P_x)_2$ superconductors, Phys. Rev. B 81 (18) (2010) 184519.
[77] A. Carrington, F. Manzano, R. Prozorov, R.W. Giannetta, N. Kameda, T. Tamegai, Evidence for surface Andreev bound states in cuprate superconductors from penetration depth measurements, Phys. Rev. Lett. 86 (2001) 1074–1077.
[78] W.N. Hardy, D.A. Bonn, D.C. Morgan, R. Liang, K. Zhang, Precision measurements of the temperature dependence of lambda in $YBa_2Cu_3O_{6.95}$: Strong evidence for nodes in the gap function, Phys. Rev. Lett. 70 (25) (1993) 3999.
[79] Y. Nakai, T. Iye, S. Kitagawa, K. Ishida, S. Kasahara, T. Shibauchi, Y. Matsuda, T. Terashima, ^{31}P and ^{75}As NMR evidence for a residual density of states at zero energy in superconducting $BaFe_2(As_{0.67}P_{0.33})_2$, Phys. Rev. B 81 (2) (2010) 020503.
[80] S. Onari, H. Kontani, Violation of Anderson's theorem for the sign-reversing *s*-wave state of iron-pnictide superconductors, Phys. Rev. Lett. 103 (17) (2009) 177001.
[81] H. Kontani, S. Onari, Orbital-fluctuation-mediated superconductivity in iron pnictides: Analysis of the five-orbital Hubbard–Holstein model, Phys. Rev. Lett. 104 (15) (2010) 157001.